



Neurokinin Receptor 1 (NK1R) Antagonist Aprepitant Enhances Hematoma Clearance by Regulating Microglial Polarization via PKC/p38MAPK/NFκB Pathway After Experimental Intracerebral Hemorrhage in Mice

Peng Jin^{1,2} · Shuixiang Deng^{1,2} · Prativa Sherchan² · Yuhui Cui² · Lei Huang^{2,3} · Gaigai Li² · Lifei Lian² · Shucui Xie² · Cameron Lenahan^{2,4} · Zachary D. Travis² · John H. Zhang^{2,3,5} · Ye Gong^{1,6} · Jiping Tang² 

Accepted: 20 June 2021 / Published online: 9 July 2021
© The American Society for Experimental NeuroTherapeutics, Inc. 2021

Abstract

Hematoma clearance is an important therapeutic target to improve outcome following intracerebral hemorrhage (ICH). Recent studies showed that Neurokinin receptor-1 (NK1R) inhibition exerts protective effects in various neurological disease models, but its role in ICH has not been explored. The objective of this study was to investigate the role of NK1R and its relation to hematoma clearance after ICH using an autologous blood injection mouse model. A total of 332 adult male CD1 mice were used. We found that the expression levels of NK1R and its endogenous ligand, substance P (SP), were significantly upregulated after ICH. Intraperitoneal administration of the NK1R selective antagonist, Aprepitant, significantly improved neurobehavior, reduced hematoma volume and hemoglobin levels after ICH, and promoted microglia polarization towards M2 phenotype. Aprepitant decreased phosphorylated PKC, p38MAPK, and NFκB p65, and downregulated M1 markers while upregulating M2 markers after ICH. Intracerebroventricular administration of the NK1R agonist, GR73632 or PKC agonist, phorbol 12-myristate 13-acetate (PMA) reversed the effects of Aprepitant. To demonstrate the upstream mediator of NK1R activation, we performed thrombin injection and found that it increased SP. Inhibiting thrombin suppressed SP and decreased M1 markers while increasing M2 microglia polarization. Thus, NK1R inhibition promoted hematoma clearance after ICH by increasing M2 microglial polarization via downregulating PKC/p38MAPK/NFκB signaling pathway, and thrombin may be a key upstream mediator of NK1R activation. Therapeutic interventions inhibiting NK1R signaling may be a new target for the treatment of ICH.

Keywords Hematoma clearance · Intracerebral hemorrhage · Microglia polarization · Neurokinin receptor-1 · Thrombin

Abbreviations

ANOVA Analysis of variance
ARRIVE Animal Research Reporting of In Vivo Experiments
DMSO Dimethyl sulfoxide
GFAP Glial fibrillary acidic protein

GPCR G-protein-coupled receptor
i.c.v Intracerebroventricular
i.p Intraperitoneal
Iba-1 Ionized calcium binding adaptor molecule 1
ICH Intracerebral hemorrhage
MAPK Mitogen-activated protein kinase
NeuN Neuronal nuclear

Peng Jin and Shuixiang Deng contributed equally to this work.

✉ Ye Gong
gong_ye@fudan.edu.cn

✉ Jiping Tang
jtang@llu.edu

¹ Department of Intensive Care Unit, Huashan Hospital, Fudan University, Shanghai 200040, China

² Department of Physiology and Pharmacology, Loma Linda University, Loma Linda, CA 92350, USA

³ Department of Neurosurgery, Loma Linda University, Loma Linda, CA 92350, USA

⁴ Burrell College of Osteopathic Medicine, Las Cruces, NM 88001, USA

⁵ Department of Anesthesiology, Loma Linda University, Loma Linda, CA 92350, USA

⁶ Department of Neurosurgery, Huashan Hospital, Fudan University, Shanghai 200040, China

NK1R	Neurokinin receptor-1
PAR1	Proteinase-activated receptor 1
PKC	Protein kinase C
PLC	Phospholipase C
PMA	Phorbol 12-myristate 13-acetate
SP	Substance P

Introduction

Intracerebral hemorrhage (ICH) is a common and devastating subtype of stroke, accounting for approximately 15% of all strokes but 50% of stroke-related mortality [1, 2, 3]. The rate of disability is high among ICH survivors, and there is currently a lack of effective neuroprotective treatment [4, 5]. Hematoma is a leading culprit that contributes to brain injury after ICH, and clinical studies have established that hematoma volume is one of the key prognostic indicators in patients with ICH [6] and neurological outcome was significantly related to hematoma clearance [7]. Therefore, effective hematoma removal is most crucial in the treatment of ICH. However, to date, surgical removal of hematoma has not shown to be an effective approach to improving outcomes in ICH patients [8]. Therefore, there is a critical need to investigate endogenous mechanisms of hematoma clearance. Modulating microglial phenotype may be a promising approach to promote hematoma clearance [9, 10].

Substance P (SP) is an undecapeptide that was first discovered in 1931 and is involved in many biological processes [11, 12]. It is produced mainly by neurons but also by some immune cells [13]. A previous study suggested that thrombin can promote the release of SP by activating proteinase-activated receptor 1 (PAR1) on the surface of neurons [14]. SP binds to specific membrane receptors on the surface of immune cells in an autocrine or paracrine manner to perform biological functions [13]. SP mediates its functions by activating the neurokinin receptor (NKR) family which is of three types, NK1R, NK2R, and NK3R [13]. Among the NKR family of receptors, NK1R, a seven-transmembrane domain G-protein-coupled receptor (GPCR) expressed by microglia, neurons, and astrocytes, displayed the highest affinity for SP [15, 16]. A growing number of studies found the therapeutic potential of targeting SP/NK1R in neurological disorders. Inhibiting NK1R played a neuroprotective role in various neurological disease models such as traumatic brain injury, cerebral infarction, encephalitis, and subarachnoid hemorrhage [17, 18, 19, 20]. However, there have been no studies evaluating the role of SP/NK1R in ICH model.

One of the major proximal pathways activated after SP binds to NK1R is phospholipase C (PLC), which promotes the formation of inositol triphosphate, thereby mobilizing intracellular stores of Ca^{2+} as well as diacylglycerol, and stimulate the phosphorylation of protein kinase C (PKC)

[21]. Phosphorylated PKC (p-PKC) can activate members of the mitogen-activated protein kinase (MAPK) cascade, including extracellular signal-regulated kinases 1/2 and p38MAPK, thereby activating NF κ B [22]. Recent studies have demonstrated that NF κ B plays an important role in microglial polarization, and inhibition of NF κ B can promote microglial transformation to M2 type [23].

In this study, we sought to investigate the role of SP and NK1R following ICH. Specifically, its effects in hematoma resolution and the underlying signaling pathway were explored. We hypothesized that inhibition of NK1R contributes to hematoma clearance by regulating microglial polarization via PKC/p38MAPK/NF κ B pathway, and thrombin derived from the hematoma may be an upstream regulator of SP release and NK1R activation. More importantly, we explored the potential therapeutic efficacy of the FDA-approved NK1R inhibitor Aprepitant in an ICH model as a preclinical approach for potential clinical translation in ICH patients.

Material and Methods

Animals

All experiments were approved by the Institutional Animal Care and Use Committee at Loma Linda University and in accordance with the National Institutes of Health (NIH) Guidelines for the Care and Use of Laboratory Animals. All animal experiments complied with the ARRIVE guidelines (<http://www.nc3rs.org.uk/arrive>). Three hundred and thirty-two male mice, age 8–12 weeks, were randomly assigned to different groups in this study. Mice were housed in the animal care facility room with controlled humidity and temperature with free access to water and food.

Sample Size Calculations

The sample size was determined using DSS Research's sample size calculation tool, assuming an α error of 5%, a β error of 20%, and a standard deviation of 25% of the mean for the data samples within each group.

Intracerebral Hemorrhage Model

ICH model was established by injection of autologous blood into the right basal ganglia as previously described [24, 25]. Mice were anesthetized with intraperitoneal injection of ketamine (100 mg/kg) and xylazine (10 mg/kg), and then placed and secured to a stereotactic frame. Artificial tear was applied to protect the eyes of the mice during surgery. The hair over the scalp was shaved, and the surgical area was wiped with an alcohol swab. A midline longitudinal incision

was made to expose the skull. Arterial blood was collected from the right femoral artery and quickly transferred into a micro-syringe (Hamilton, NV, USA). The needle of a Hamilton syringe was inserted through a burr hole into the right basal ganglia at coordinates: 0.2 mm anterior, 2.2 mm lateral, and 3.5 mm ventral to the bregma. A total volume of 30 μ l blood was infused at a rate of 3 μ l/min with an infusion pump (Harvard Apparatus, MA, USA). The syringe was left in place for 10 min after finishing injection. Skin incision was closed after the burr hole was sealed with bone wax. Sterile 0.9% NaCl solution 0.4 ml was administered by intraperitoneal injection to ensure hydration. Mice were closely monitored until fully awake from anesthesia. The mice in sham group received identical procedures including blood draw and micro-syringe insertion, except for a real injection.

Drug Administration

The selective NK1R antagonist Aprepitant (Bio-Techne Corporation, MN, USA) was dissolved in 10% DMSO at a concentration of 30 mg/ml and administered by intraperitoneal injection at 1 h after ICH. Three different doses [20] (40, 120, 360 mg/kg) of Aprepitant were tested. An equivalent volume of 10% DMSO (100 μ l) was administered intraperitoneally to the control group. GR73632 (Bio-Techne Corporation, MN, USA), a specific NK1R agonist, and PMA (Sigma Aldrich, MO, USA), a PKC activator, were injected into the left lateral ventricle by intracerebroventricular administration (i.c.v.). GR73632 was dissolved in DMSO to a final concentration of 100 μ g/1200 μ l, which was administered at a dose of 1 μ g/mice 1 h after ICH [26]. PMA was also dissolved in DMSO and then administered at a dose of 0.1 nmol/mice at 1 h after ICH [27, 28]. An equivalent volume of DMSO (1.2 μ l) was administered by i.c.v. to the control group.

Intracerebroventricular Injection

Intracerebroventricular injection was performed as previously described [29]. Briefly, a cranial burr hole was drilled at the following coordinates relative to bregma: 0.3 mm posterior, 1.0 mm lateral, and 2.3 mm deep. The needle of a 10- μ l Hamilton syringe was inserted into the left ventricle through the burr hole, and infusion was performed at a rate of 2 μ l/min. At the end of infusion, the needle was left in place for an additional 8 min and then removed over 3 min [30].

Thrombin Injection

Thrombin injection was performed following a previously published method from our laboratory [31]. Animals were anesthetized and then fixed to a stereotactic frame. Thrombin

was injected into right basal ganglia using the same coordinates as described above for autologous blood injection model. Thrombin (Sigma Aldrich, MO, USA) was dissolved in sterilized PBS to a final concentration of 1 μ l/ μ l, and then injected into the right basal ganglia at a dose of 5 μ l/mice and a rate of 2 μ l/min. Animals in the control group were given 5 μ l of PBS following the same procedure.

Experiment Design

Five separate experiments were conducted as follows (Fig. S1). In order to exclude the influence of human interference and human subjectivity on the experimental results, a double-blind method was used in this experiment.

Experiment 1

To evaluate endogenous expression of NK1R and its ligand SP, 42 mice were randomly divided into seven groups to perform western blot: sham, ICH-3 h, ICH-6 h, ICH-12 h, ICH-24 h, ICH-72 h, and ICH-7d (n = 6/group). In addition, the cellular co-localization of NK1R was evaluated using double immunofluorescence staining in sham and ICH-24 h group (n = 2/group).

Experiment 2

To assess the effect of inhibiting NK1R on ICH outcomes, the FDA-approved specific NK1R inhibitor Aprepitant was administered intraperitoneally 1 h post-ICH. Mice were randomly divided into five groups: sham, ICH + Vehicle (DMSO), ICH + Aprepitant (40 mg/kg), ICH + Aprepitant (120 mg/kg), and ICH + Aprepitant (360 mg/kg) (n = 6/group). Behavioral tests were performed 24 h after ICH following which mice were sacrificed to assess brain edema, hematoma volume, and hemoglobin levels. Next, post-ICH outcomes at 72 h and 7 days were evaluated using the best dose of Aprepitant. Mice were randomly divided into three groups: sham, ICH + Vehicle (DMSO), and ICH + Aprepitant (best dose) (n = 6/group). Furthermore, to assess whether delayed administration was still effective, another 12 mice were selected and divided into 2 groups: ICH + Aprepitant (best dose, 3 h post-ICH) and ICH + Aprepitant (best dose, 6 h post-ICH); outcomes were evaluated at 72 h after ICH. To assess the effect of NK1R inhibition on microglial polarization, brain samples were harvested for immunofluorescence staining 72 h after ICH. To further confirm the role of NK1R, 18 mice were randomly divided into three groups: sham, ICH + DMSO (i.c.v.), and ICH + GR73632 (i.c.v.) (n = 6/group). The specific NK1R agonist GR73632 was administered intracerebroventricularly 1 h after ICH, and hematoma volume and hemoglobin level were evaluated at 72 h.

Experiment 3

To assess therapeutic effect of Aprepitant on the long-term outcomes after ICH, 45 mice were divided into 3 groups: sham, ICH + vehicle, and ICH + Aprepitant (120 mg/kg). Foot-fault test and rotarod test were conducted on days 14 and 21 after ICH. Morris water maze was performed at 23 to 28 days after ICH following which mice were sacrificed and brain samples were harvested for Nissl staining.

Experiment 4

To assess the potential molecular pathway of NK1R in microglial polarization, the specific NK1R agonist, GR73632, and a specific PKC agonist, PMA, were administered to mice that received Aprepitant. Thirty-six mice were divided into 6 groups: sham, ICH + vehicle (DMSO), ICH + Aprepitant, ICH + Aprepitant + DMSO, ICH + Aprepitant + GR73632, and ICH + Aprepitant + PMA. Mice were sacrificed 72 h after ICH to collect brain samples for western blot to detect pathway proteins and the expression of M1, M2 markers.

Experiment 5

To investigate the upstream regulator of NK1R activation, thirty mice were randomly divided into five groups: sham, thrombin + PBS, thrombin + hirudin, thrombin + DMSO, and thrombin + Aprepitant. Thrombin as well as its specific inhibitor, hirudin, was injected into the right basal ganglia of naïve mice. Western blot was performed 72 h after surgery. To further verify the role of thrombin in ICH model, 30 mice were divided into five groups: sham, ICH + PBS, ICH + hirudin, ICH + hirudin + DMSO, and ICH + hirudin + GR73632. Garcia score test, corner turn test, forelimb placement test, and western blot were conducted at 72 h post-ICH.

Neurobehavioral Tests

Neurological outcomes were assessed using modified Garcia test, corner turn test, and forelimb placement test by the researcher who was blinded to the experimental groups and treatments at different time points after ICH as previously described [30, 32]. Modified Garcia test consisted of seven separate parameters including spontaneous activity, vibrissae touch, climbing, response to lateral stroking, limb symmetry, forelimb walking, and lateral turning. Each parameter was given a score ranging from 0 to 3, with a maximum score of 21 indicating no deficits. In the corner turn test, mice were allowed to advance to a 30° angle and exit by turning either left or right. The choice of turns out of 10 trials was recorded, and the left turn % score was calculated as the number of left turns/all trials \times 100. The forelimb

placement test evaluated responsiveness to vibrissae stimulation. Mice were slowly moved up and down at the height of the table so that the vibrissae lightly touched the tabletop. The left forelimb placement % score was calculated as a percentage of 10 trials in which the left forelimb was successfully placed on the tabletop.

Morris water maze test was performed on days 23 to 28 post-ICH as described previously [33, 34]. The experiment was conducted in a circular pool with a 10-cm escape platform that was submerged 1 cm below the surface of water. The pool was divided into 4 quadrants, and mice were allowed to swim for up to 60 s starting at different quadrants during each trial and allowed to stay on the platform for 5 s. On day 28, the platform was removed for probe trial. Swim distance, escape latency, and time spent in the probe quadrant were recorded by a computerized tracking system (San Diego Instruments Inc., CA, USA).

Foot fault test and rotarod test were performed on days 14 and 21 post-ICH as previously described [35]. In the foot fault test, mice moved along a horizontal grid (20 cm \times 100 cm) for 2 min. The number of left forelimb footfaults was counted. In rotarod test, mice were placed on an accelerated rotating horizontal cylinder at a starting speed of 5 rpm with a regular increase in speed. Three trials were performed and the mean time of falling latency was recorded.

Measurement of Brain Water Content

The wet/dry weight method was performed to measure brain water content as previously described [36]. After being fully anesthetized, the mice brains were rapidly removed and divided into five parts: right basal ganglia, left basal ganglia, right cortex, left cortex, and cerebellum. Brain samples were weighed with an electronic analytical balance (APX-60, Denver Instrument, NY) to get the wet weight. The samples were then dried at 100 °C for 24 h to obtain the dry weight. Brain water content (%) was calculated as [(wet weight—dry weight)/wet weight] \times 100%.

Hematoma Volume Assessment

After being fully anesthetized with isoflurane, mice were transcardially perfused with ice-cold PBS. Fresh 1-mm brain slices were prepared according to the standard procedure developed by Chang et al. [37]. Images of the brain slices were digitized by camera and analyzed using Image J software (NIH, Bethesda, USA).

Hemoglobin Assay

Hemoglobin assay was conducted as previously described [38]. After homogenization and ultrasonic lysis of the

ipsilateral brain specimens, the samples were centrifuged and supernatant was obtained. Drabkin's reagent (Sigma-Aldrich, MO, USA) 0.4 mL was added to 0.1 mL of supernatant and allowed to react for 15 min at room temperature. The optical density was then measured at 550 nm using a spectrophotometer (Thermo Fisher Scientific, MA, USA). The data was calculated as a ratio to sham, with the default value 1 for sham as in the previous study [29].

Western Blot

Western blotting was conducted as previously described [39, 40]. Briefly, after transcardiac perfusion with ice-cold PBS, brain tissue was quickly removed and stored at -80°C for later analysis. Brain samples were homogenized in RIPA lysis buffer (Santa Cruz Biotechnology, CA, USA) and centrifuged at 14,000 g for 30 min at 4°C following which the supernatant was collected. Protein concentration in the supernatants was measured using a detergent-compatible assay (DC Protein Assay, Bio-Rad Laboratories, CA, USA). Equal amounts of proteins were loaded on SDS-PAGE gels, separated by electrophoresis and transferred to nitrocellulose membranes. After blocking with 5% nonfat milk (Bio-Rad Laboratories, CA, USA) for 2 h at room temperature, the membranes were incubated with following primary antibodies overnight at 4°C : anti-substance P (1:200, Biorbyt, UK), anti-NK1R (1:500, Santa Cruz Biotechnology, CA, USA), anti-PKC (1:2000, Santa Cruz Biotechnology, CA, USA), anti-p-PKC (1:500, Santa Cruz Biotechnology, CA, USA); anti-p38MAPK (1:2000, Cell Signaling Technology, MA, USA); anti-p-p38MAPK (1:500, Cell Signaling Technology, MA, USA); anti-NF κ B p65 (1:250, Cell Signaling Technology, MA, USA); anti-p-NF κ B p65 (1:200, Cell Signaling Technology, MA, USA); anti-CD206 (1:500, Abcam, MA, USA); anti-CD163 (1:1000, Santa Cruz Biotechnology, CA, USA); anti-CD16 (1:1000, Abcam, MA, USA); anti-CD86 (1:2000, Santa Cruz Biotechnology, CA, USA); and anti- β actin (1:5000, Santa Cruz Biotechnology, CA, USA). The following day, membranes were incubated with an appropriate secondary antibody (1:3000, Santa Cruz Biotechnology, CA, USA) at room temperature for 2 h. The bands were visualized after the membranes were subjected to ECL Plus kit and then exposed to X-ray films. The band density was quantified using Image J (NIH, Bethesda, USA). The results were standardized using β -actin as an internal control.

Histology

Mice were deeply anesthetized with isoflurane and perfused transcardially with PBS followed by 10% formalin. Brain samples were harvested and placed in 10% formalin for 1 day and in 30% sucrose solution for 3 days. Subsequently, the brains were frozen in OCT and cut into 10- μm -thick coronal

sections using a cryostat (CM3050S; Leica Microsystems, Germany). Brain sections were used for immunofluorescence and Nissl staining.

Immunofluorescence Staining

Double immunofluorescence staining was conducted as previously described [41]. The slides were washed 3 times with 0.01 M PBS for 10 min each, then incubated in 0.3% Triton X-100 for 10 min, followed by incubation with 5% donkey serum at room temperature for 2 h. The brain sections were then incubated overnight at 4°C with primary antibodies including: anti-NK1R (1:50, Santa Cruz Biotechnology, CA, USA), anti-NeuN (1:100, Abcam, MA, USA), anti-GFAP (1:100, Abcam, MA, USA), and anti-Iba-1 (1:100, Abcam, MA, USA), anti-CD206 (1:50, Abcam, MA, USA), anti-CD163 (1:25, Santa Cruz Biotechnology, CA, USA), anti-CD16 (1:100, Abcam, MA, USA), and anti-CD86 (1:100, Santa Cruz Biotechnology, CA, USA). Sections were then washed with PBS (12 \times 5 min) and incubated with the corresponding secondary antibody (1:100, Jackson Immuno Research, PA, USA) for 1 h at room temperature, protected from light, visualized, and photographed with a fluorescence microscope (Leica Microsystems, Germany) at $\times 400$ magnification.

Nissl Staining

Nissl staining was performed as previously described [42]. The sections were dehydrated successively in 95% and 70% FLEX (Thermo Fisher Scientific, MA, USA) for 1 min, then rinsed twice with distilled water for 30 s. Next, the sections were stained in 0.5% cresyl violet (Sigma Aldrich, MO, USA) for 1.5 min, rinsed again with distilled water for 30 s, and then placed in 100% FLEX and xylene for 1 min (twice each). Finally, the sections were mounted with DPX (Sigma Aldrich, MO, USA) and imaged with a microscope (BX51, Olympus, Japan). Neuronal degeneration in the hippocampus CA1, CA3, and DG regions were observed and quantified.

Statistical Analysis

All data in this study were expressed as mean \pm standard deviation (SD). The data were analyzed using SPSS Statistics 20 and GraphPad Prism 8. Multiple comparisons were analyzed using one-way ANOVA and post hoc Bonferroni test. Two-way ANOVA, followed by Tukey post hoc test, was used to compare the changes according to the different levels of multiple categorical variables (brain water content, long-term neurological function). Data were screened for normality using the Shapiro–Wilk test. Since data were not normally distributed, the between-group post-outcome

differences were analyzed with non-parametric test. $p < 0.05$ was considered to be statistically significant.

Results

Mortality and Exclusion

A total of 332 mice were used in this study, out of which 59 were in the sham group. No mice died in the sham group and 4 died in the ICH group, so the overall mortality rate was 1.20% (4/332). A total of 3 ICH mice were excluded because they did not show neurological deficits after surgery. (After euthanizing these mice, we found that there was no hematoma in their brains.) Details of animals used are listed in Table S1.

Expression of SP and NK1R Increased in a Time-Dependent Manner After ICH

Ipsilateral brain hemisphere samples were collected for western blot in sham and at 3 h, 6 h, 12 h, 24 h, 72 h, and 7 days after ICH. The results showed that NK1R and its ligand SP rapidly increased compared to sham group, and peaked around 24 h after ICH and started decreasing thereafter. On day 7 post-ICH, NK1R was almost back to normal levels whereas SP had decreased but remained significantly higher than in sham group (Fig. 1A–C). Double immunofluorescence staining showed that NK1R was mainly expressed in microglia and neurons with minor expressions noted in astrocytes (Fig. 1D).

Aprepitant Treatment Reduced Brain Edema and Neurobehavioral Deficits But Did Not Affect Hematoma Volume or Hemoglobin Levels 24 h After ICH

We evaluated the efficacy of three different doses of Aprepitant (40 mg/kg, 120 mg/kg, 360 mg/kg) to determine the optimal dose. The ICH groups had significantly increased brain water content in ipsilateral cortex and basal ganglia as well as severe neurological deficits compared to the sham group. All doses of Aprepitant significantly reduced brain water content in the ipsilateral basal ganglia 24 h after ICH compared to vehicle group, but only the middle dose (120 mg/kg) reduced water content in the ipsilateral cortex (Fig. 2D). In neurobehavioral tests, the middle dose group also performed better 24 h after ICH (Fig. 2E–G). Aprepitant middle dose treatment showed a trend towards reducing hematoma volume compared to the vehicle group, but there was no significant difference (Fig. 2A–C). Based on these

results, Aprepitant 120 mg/kg dose was used for the rest of the experiments in this study.

Aprepitant Treatment Reduced Brain Edema, Hematoma Volume, Hemoglobin Levels, and Improved Neurological Function 72 h After ICH

Aprepitant 120 mg/kg was used to evaluate outcomes 72 h after ICH. The results showed that compared with ICH + vehicle group, ICH + Aprepitant group had significantly lower brain water content (Fig. 3D). Aprepitant-treated mice obtained higher scores in both modified Garcia test and forelimb placement test compared to vehicle group (Fig. 3E–G). Aprepitant significantly reduced hematoma volume and hemoglobin levels 72 h after ICH compared to the vehicle group. To assess whether delayed Aprepitant treatment was still effective, we evaluated the effects of Aprepitant administered 3-h and 6-h post-ICH, which also showed positive effects in reducing hematoma volume and hemoglobin levels 72 h after ICH (Fig. 3A–C). To further confirm the role of the NK1R signaling pathway in hematoma clearance, we evaluated the effects of NK1R agonist GR73632. The administration of GR73632 significantly increased hematoma volume and hemoglobin levels compared to vehicle group 72 h after ICH (Fig. 3H–J).

Aprepitant Treatment Reduced Hematoma Volume, Hemoglobin Levels, and Improved Neurological Function 7 Days After ICH

By day 7, the hematoma in ICH + vehicle group had become very small and was almost completely absorbed in the ICH + Aprepitant treatment group. Similarly, behavioral tests showed that ICH mice with Aprepitant treatment performed better than vehicle (Fig. 4A–F).

Aprepitant Reduced Hippocampal Neuronal Degeneration and Improved Long-Term Neurobehavioral Outcomes After ICH

Nissl staining was performed to assess neuronal degeneration in the hippocampus which showed a greater number of dark Nissl bodies in the CA1, CA3, and DG regions of the hippocampus in ICH mice than in sham group. Aprepitant treatment decreased the number of dark Nissl bodies in these regions (Fig. 5A–B). Morris water maze test showed that ICH mice had significantly longer swimming distance and escape latency compared to sham group, and Aprepitant significantly reduced swimming distance and escape

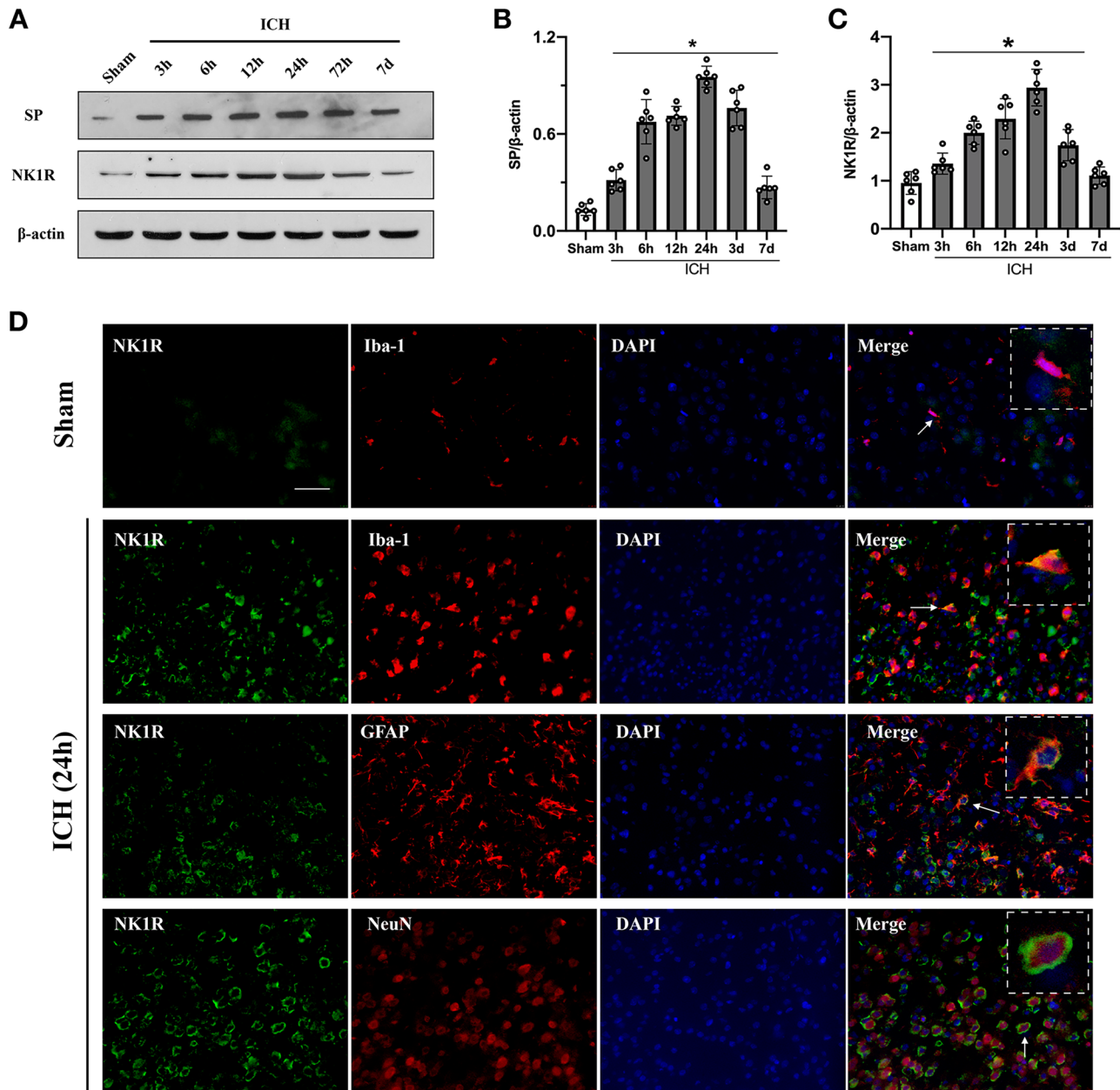


Fig. 1 Time course expression of substance P and NK1R after ICH, and cellular location of NK1R after ICH. **A–C** Representative western blot bands and quantitative analyses of substance P (SP) and NK1R expression in the ipsilateral hemisphere in sham and ICH mice. Data was expressed as mean \pm SD. * $p < 0.05$ vs sham; one-way

ANOVA, Tukey test, $n = 6$ /group. **D** Representative pictures of immunofluorescence staining for NK1R (green) expression in microglia (Iba-1, red), neurons (NeuN, red), and astrocytes (GFAP, red) in sham group and the peri-hematoma area 24 h after ICH. Scale bar = 50 μ m. $n = 2$

latency in blocks 4 and 5. In the probe test, Aprepitant treatment increased the duration of time ICH mice spent in the probe quadrant (Fig. 5C–F). In the foot fault test, left foot fault was significantly increased after ICH compared to sham, and in rotarod test, the latency to fall was shorter after ICH compared to sham. Aprepitant treated animals showed significant improvement in both tests (Fig. 5G–H).

Aprepitant Treatment Promoted M2 Polarization at 72 h After ICH

To assess the effects of NK1R on microglial polarization, we evaluated two classical M1 markers CD16 and CD86 and two phagocytosis-associated M2 markers CD206 and CD163 to co-localize with microglia.

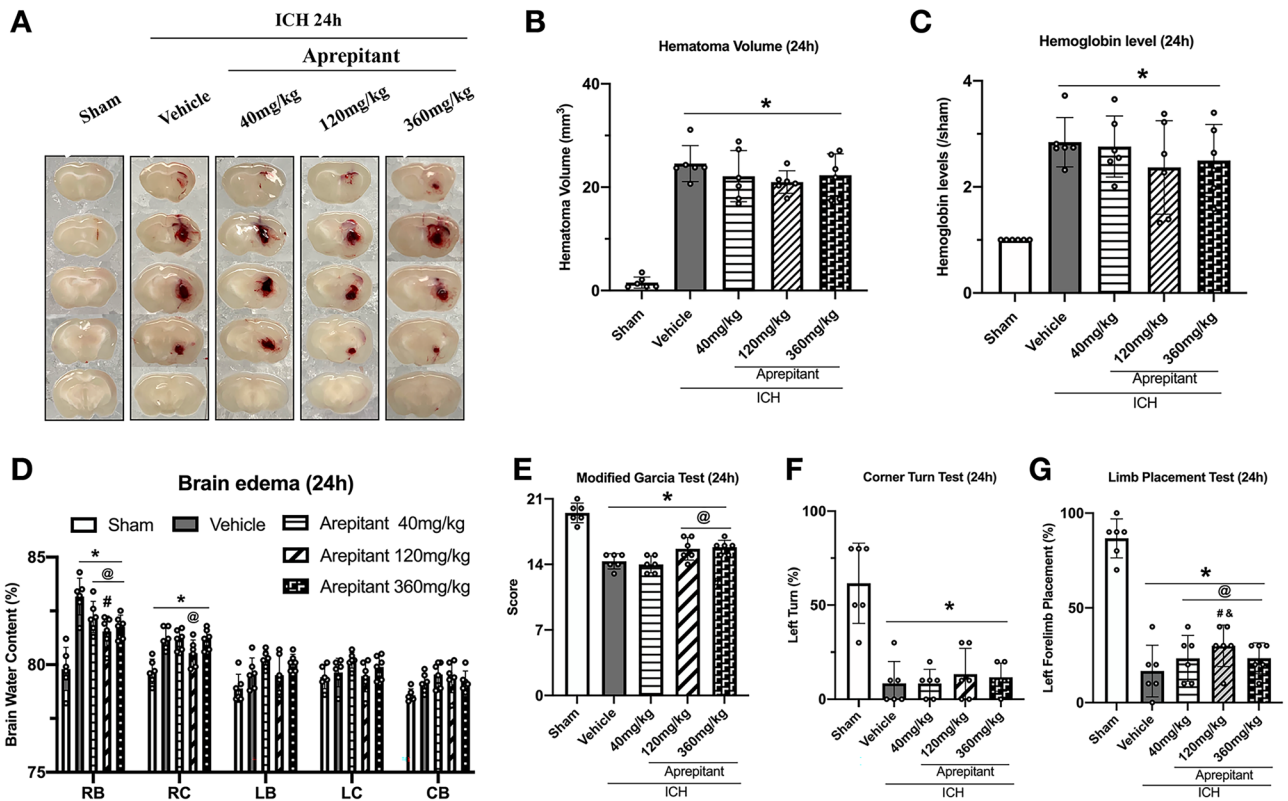


Fig. 2 The effects of Aprepitant administration on hematoma volume, hemoglobin levels, brain edema, and neurobehavior tests at 24-h post-ICH. **A** Representative photograph of brain sections, **B–C** quantitative analyses of hematoma volume and hemoglobin level, **D** brain water content, **E** modified Garcia test, **F** corner turn test, and

G forelimb placement test at 24 h after ICH. Data was represented as mean \pm SD. * $p < 0.05$ vs sham; @ $p < 0.05$ vs ICH + vehicle; # $p < 0.05$ vs ICH + Aprepitant 40 mg/kg; & $p < 0.05$ vs Aprepitant 360 mg/kg. One-way ANOVA, Tukey test, $n = 6$ /group. RB right basal ganglia, RC right cortex, LB left basal ganglia, LC left cortex, CB cerebellum

Double immunofluorescence results showed that microglia morphology remained resting and ramified in the sham group. A large number of microglia were activated 72 h after ICH, and in the absence of intervention, they comprised mostly of M1 phenotype and to a lesser extent M2 phenotype. Compared to the ICH + vehicle group, Aprepitant treatment significantly decreased the number of CD16 and CD86-positive microglia and significantly increased the number of CD206 and CD163-positive microglia (Fig. 6A–F). These results suggested that NK1R inhibitor Aprepitant promoted M2 polarization after ICH.

Activation of NK1R or PKC Abolished the Effects of Aprepitant Post-ICH

Western blot was conducted to evaluate the expression of NK1R and downstream PKC-p38MAPK-NF κ B signaling pathway, and microglia markers at 72 h after ICH. The results showed increased expression of NK1R; increased

phosphorylation of potential downstream pathway proteins PKC, p38MAPK, and NF κ B p65; and increased M1 classical markers CD16, CD86, and phagocytosis-related M2 markers CD206 and CD163 at 72 h after ICH (Fig. 7A–I). Compared with ICH + vehicle group, Aprepitant did not change the expression of NK1R but it decreased the expression of downstream pathway proteins and M1 phenotype markers while significantly increasing M2 phenotype markers (Fig. 7A–I). These changes were reversed with intracerebroventricular injection of NK1R agonist GR73632 or PMA, a specific agonist of PKC when administered to ICH mice that received Aprepitant. The phosphorylation of PKC, p38MAPK, and NF κ B p65 and M1 phenotype markers were increased, while M2 markers decreased in ICH + Aprepitant + GR73632 and ICH + Aprepitant + PMA groups compared with ICH + Aprepitant + DMSO group (Fig. 7A–I). These results suggested that Aprepitant regulated microglial phenotype transformation by promoting M2 phenotype via inhibiting NK1R and downstream PKC-p38 MAPK-NF κ B signaling pathway.

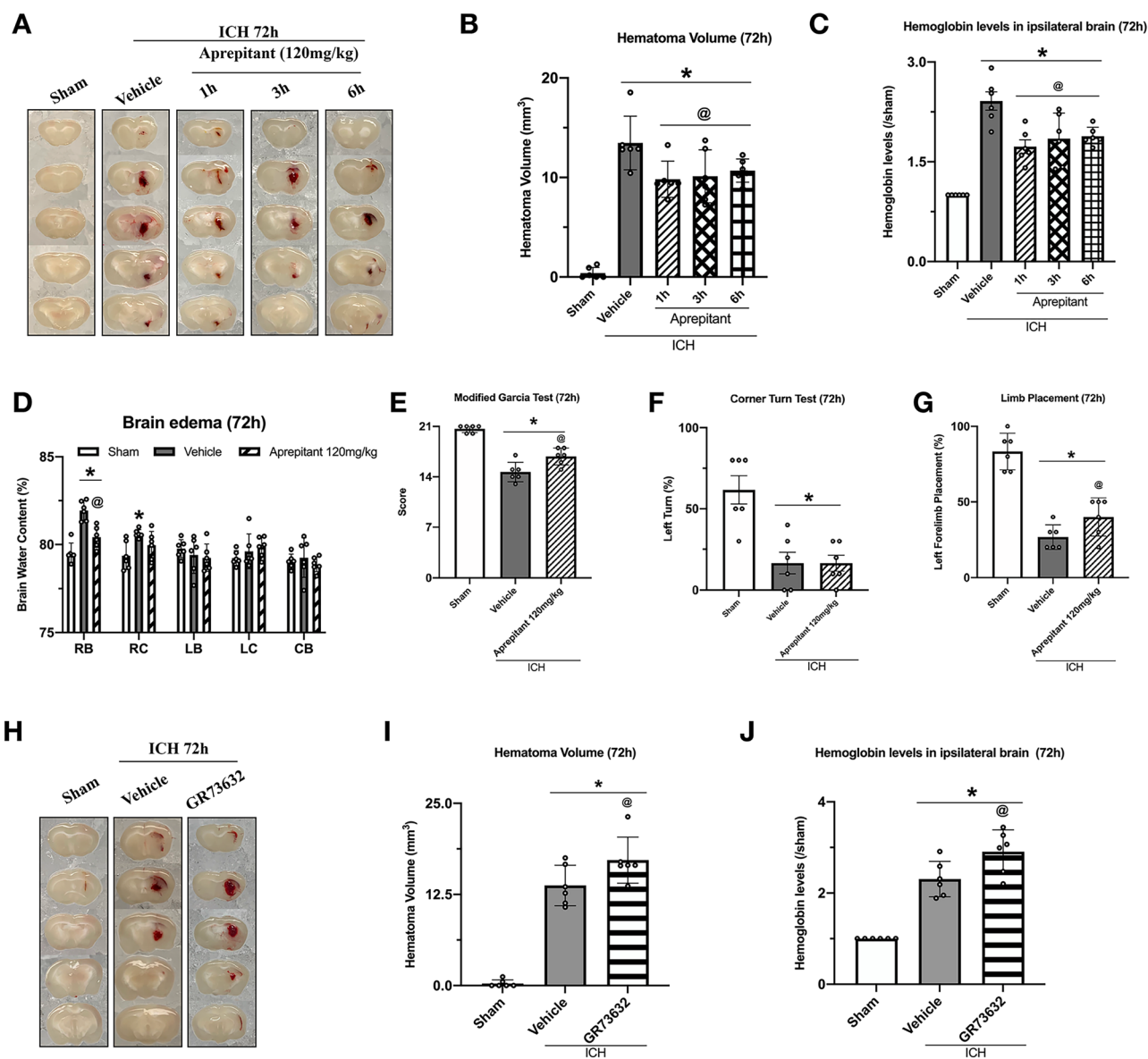


Fig. 3 Effects of Aprepitant administration at different time-points after ICH and activation of NK1R by GR73632 on ICH outcomes evaluated at 72-h post-ICH. **A, H** Representative photograph of brain sections, **B–C, I–J** quantitative analyses of hematoma volume and hemoglobin level, **D** brain water content, **E** modified Garcia test, **F**

corner turn test, and **G** forelimb placement test at 72 h after ICH. Data was represented as mean \pm SD. * $p < 0.05$ vs sham; @ $p < 0.05$ vs ICH + vehicle. One-way ANOVA, Tukey test, $n = 6$ /group. RB right basal ganglia, RC right cortex, LB left basal ganglia, LC left cortex, CB cerebellum

Thrombin Regulated Microglial Polarization by Promoting the Release of SP

To explore the upstream regulation of NK1R, we used a thrombin-injection model and hirudin; a specific thrombin inhibitor was co-injected into the right basal ganglia of naïve mice. Thrombin injection significantly increased the release of SP compared to sham group, which was significantly reduced with hirudin co-injection. Furthermore, the expression of M1 markers CD16 and CD86 was decreased and M2 markers CD206 and CD163 increased when hirudin was co-injected with

thrombin (Fig. 8A–B). These results suggested that thrombin regulated microglia polarization by promoting the release of SP.

Aprepitant Treatment Modulated Thrombin-Induced Changes in Microglial Polarization

To further confirm the regulatory relationship between thrombin and NK1R, we administered Aprepitant to the thrombin-injection model. The results showed that Aprepitant did not alter the release of SP but reversed thrombin-induced changes

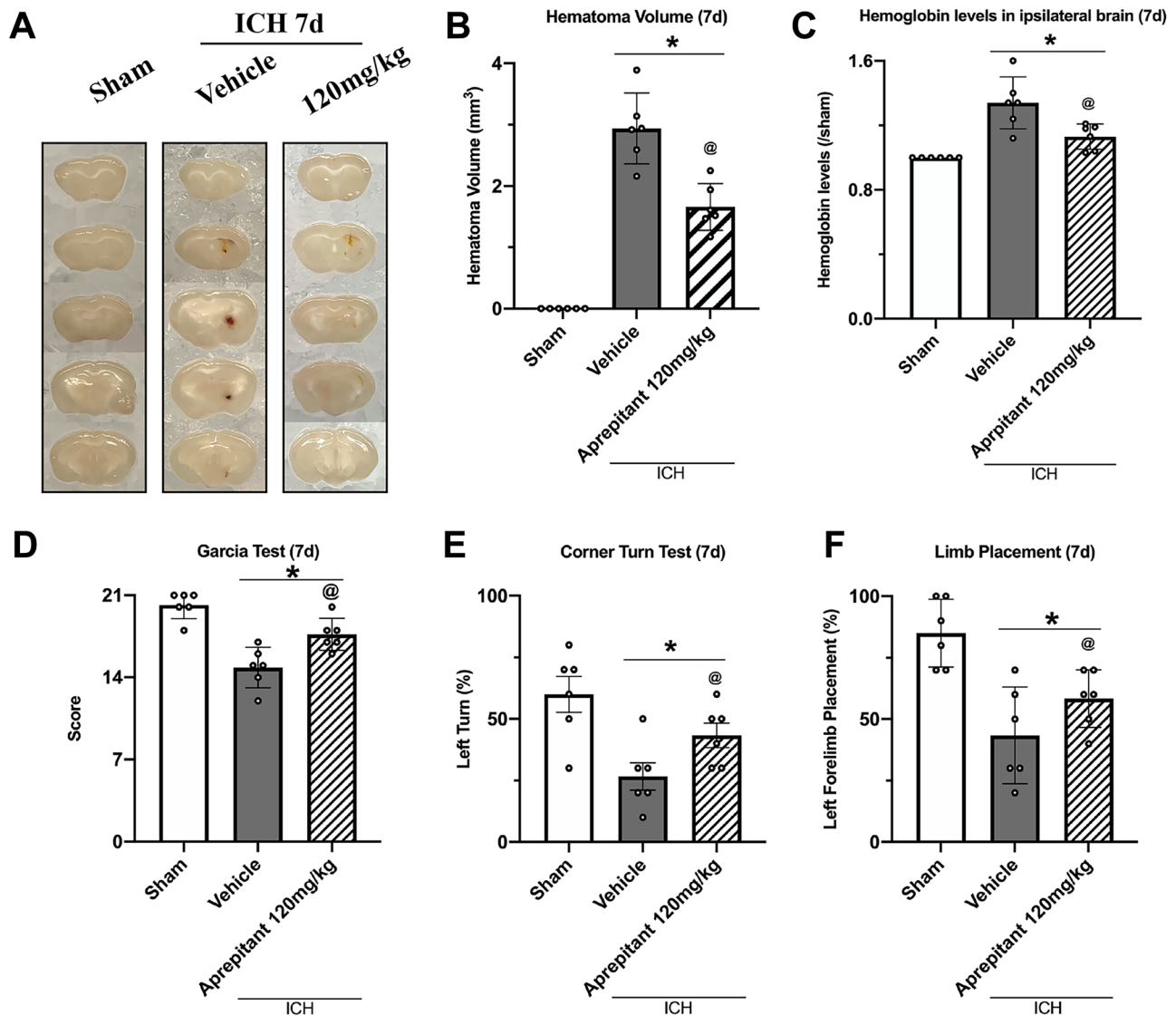


Fig. 4 The effects of Aprepitant administration on hematoma volume, hemoglobin levels, and neurobehavioral tests at 7 days post-ICH. **A** Representative photograph of brain sections, **B–C** quantitative analyses of hematoma volume and hemoglobin level, **D** Modified Garcia

test, **E** corner turn test, and **F** forelimb placement test at 7 days after ICH. * $p < 0.05$ vs sham; @ $p < 0.05$ vs ICH + vehicle. Error bars are represented as mean \pm SD. One-way ANOVA, Tukey's test, $n = 6$ /group

in microglial polarization. The expression of CD206 and CD163 was increased, and the expression of CD16 and CD86 decreased in thrombin + Aprepitant group compared with thrombin + DMSO group (Fig. 8C–D). These results suggested that inhibition of NK1R reversed thrombin induced M1 microglial polarization.

Activation of NK1R with GR73632 Abolished Neuroprotective Effects of Hirudin After ICH

We administered hirudin and NK1R agonist GR73632 to ICH mice. The results showed that hirudin significantly decreased the expression of SP and promoted microglial

transformation to M2 phenotype 72 h after ICH (Fig. 8E–F). Furthermore, compared with ICH + hirudin + DMSO group, the expression of CD16 and CD86 increased, while the expression of CD206 and CD163 was decreased in ICH + hirudin co-injection + GR73632 group (Fig. 8E–F). Hirudin improved the performance in neurobehavioral tests 72 h after ICH, and neurological deficits were worsened in the ICH + hirudin + GR73632 group compared with ICH + hirudin + DMSO group (Fig. 8G–I). These results showed that the neuroprotective effects exerted by hirudin were achieved, in part, by inhibiting NK1R activation. These findings suggested that thrombin may be upstream of NK1R activation.

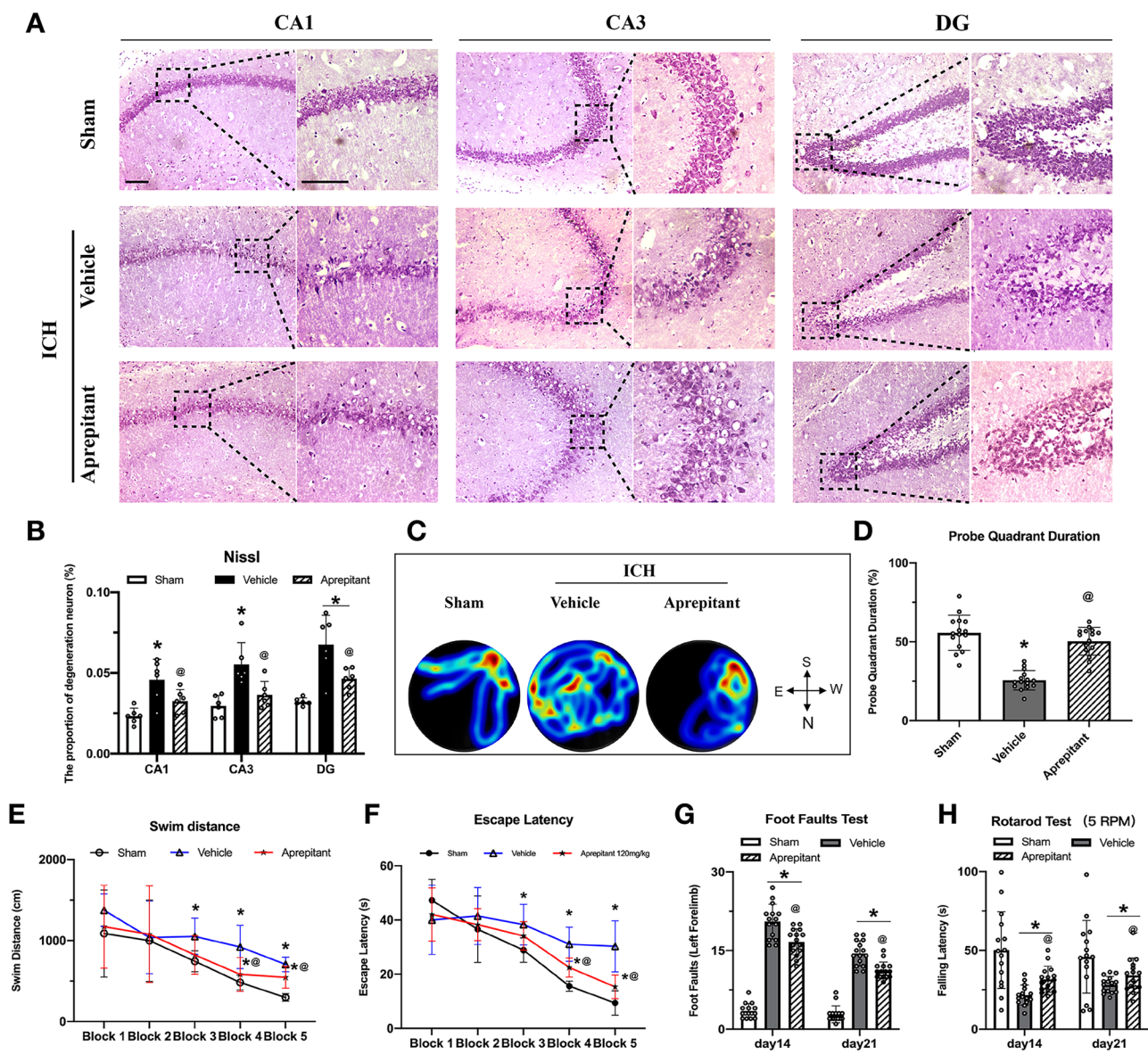


Fig. 5 Effects of NK1R inhibition with Aprepitant on long-term outcomes after ICH. **A–B** Nissl staining representative micrographs and neuronal quantification of the hippocampal CA1, CA3, and DG regions; **C** water maze test representative heat maps during probe trial; **D** probe quadrant duration on day 28 after ICH; **E** swimming distance and **F** escape latency on days 23 to 27 after ICH; and **G**

foot fault test and **H** rotarod test at second and third week post-ICH. Data was represented as mean \pm SD. * $p < 0.05$ vs sham; @ $p < 0.05$ vs ICH+vehicle group; One-way ANOVA, Tukey post hoc test (**B** and **D**). Two-way repeated measures ANOVA, Tukey post hoc test (**E–H**), $n = 15/\text{group}$

Discussion

Intracerebral hemorrhage is a devastating stroke with high morbidity and mortality [43]. Following ICH, the hematoma itself can lead to primary damage due to mechanical destruction and intracranial pressure elevation, whereas blood components such as thrombin can cause secondary brain damage. Therefore, hematoma removal is a key target for the treatment of cerebral hemorrhage [44, 45]. In the present study, we investigated for the first time the role of SP/NK1R system and its role in

hematoma clearance following ICH injury. Our results showed that NK1R and its ligand SP were rapidly elevated after ICH. The NK1R selective antagonist, Aprepitant, promoted the differentiation of microglia into M2 phenotype which contributed to reduce hematoma volume and lower hemoglobin levels after ICH, thereby improving short-term and long-term neurological outcomes. Our results suggest that NK1R signaling may contribute to microglia polarization at least partly via PKC/p38MAPK/NF κ B pathway. Furthermore, thrombin may be an upstream regulator of NK1R activation after ICH.

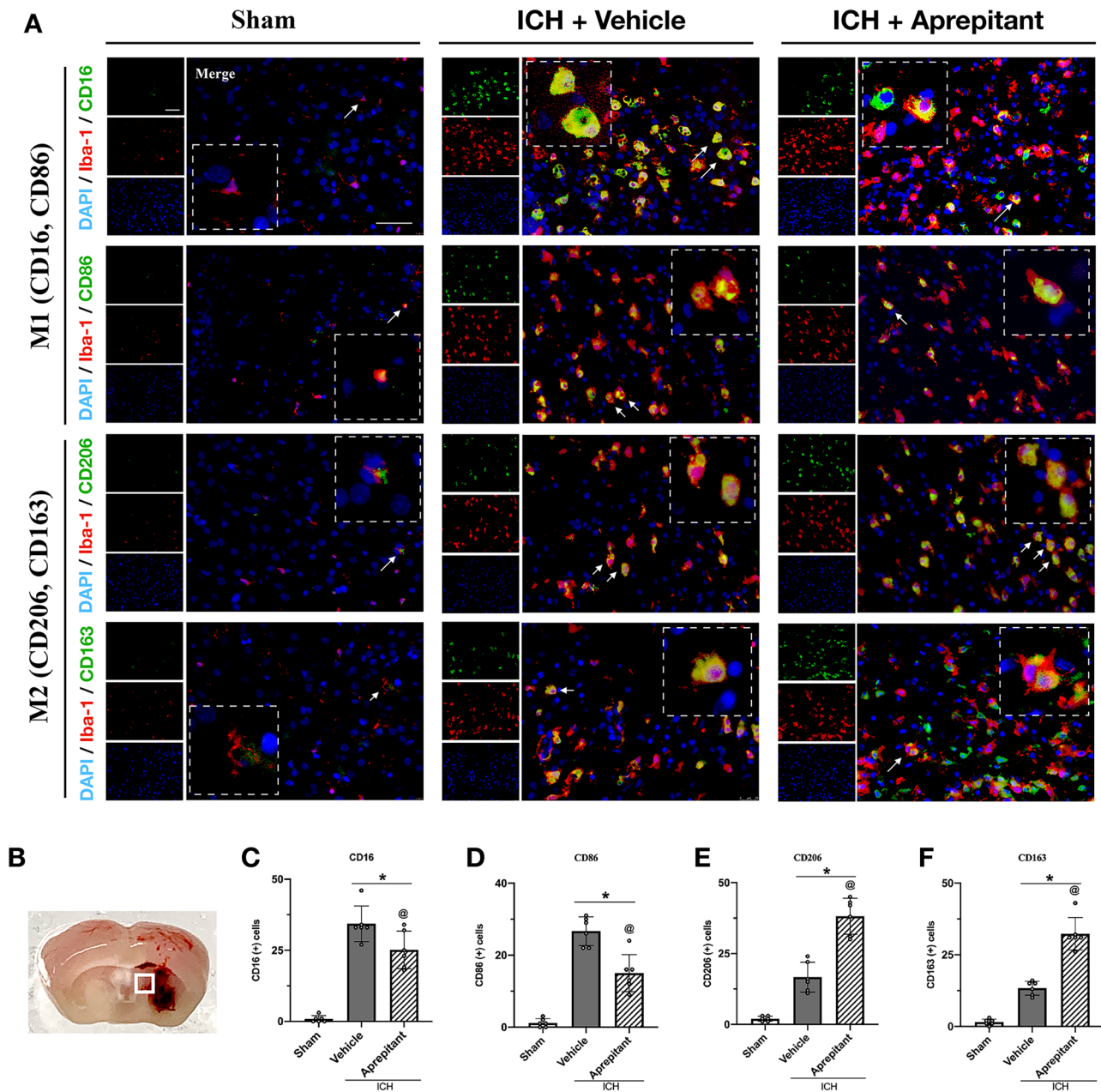


Fig. 6 Effects of NK1R inhibition with Aprepitant on microglia polarization at 72 h after ICH. **A** Representative images of immunofluorescence staining of CD16 (green), CD86 (green), CD206 (green), and CD163 (green) with Iba-1 (red) in the perihematomal area at 72 h after ICH; **B** schematic illustration of brain tissue shows

the perihematomal region depicted with a white square; **C–F** quantitative analyses of CD16, CD86, CD206, and CD163-positive cells in the perihematomal area at 72 h after ICH. Data was represented as mean ± SD. * $p < 0.05$ vs sham, @ $p < 0.05$ vs ICH + vehicle. One-way ANOVA, Tukey test, $n = 6$ /group

SP is a member of the tachykinin neuropeptide family that exerts its biological effects by binding to high-affinity neurokinin 1 receptor [13]. NK1R is a G protein-coupled receptor that is expressed in neurons, microglia, astrocytes, and other immune cells [46]. In a traumatic brain injury model, NK1R expression was found to be significantly elevated after brain injury [18]. Consistent with these findings, we found that NK1R expression significantly increased 24 h after ICH and it was mainly

expressed in microglia and neurons with minor expression in astrocytes. The fact that inhibition of NK1R can exert neuroprotective effects is not a new concept. Previous studies focused on the relationship between NK1R and neuroinflammation, and inhibition of NK1R was found to protect the blood–brain barrier [47]. However, our study demonstrates for the first time that inhibition of NK1R promoted hematoma clearance and thus improved short- and long-term outcomes following ICH in mice.

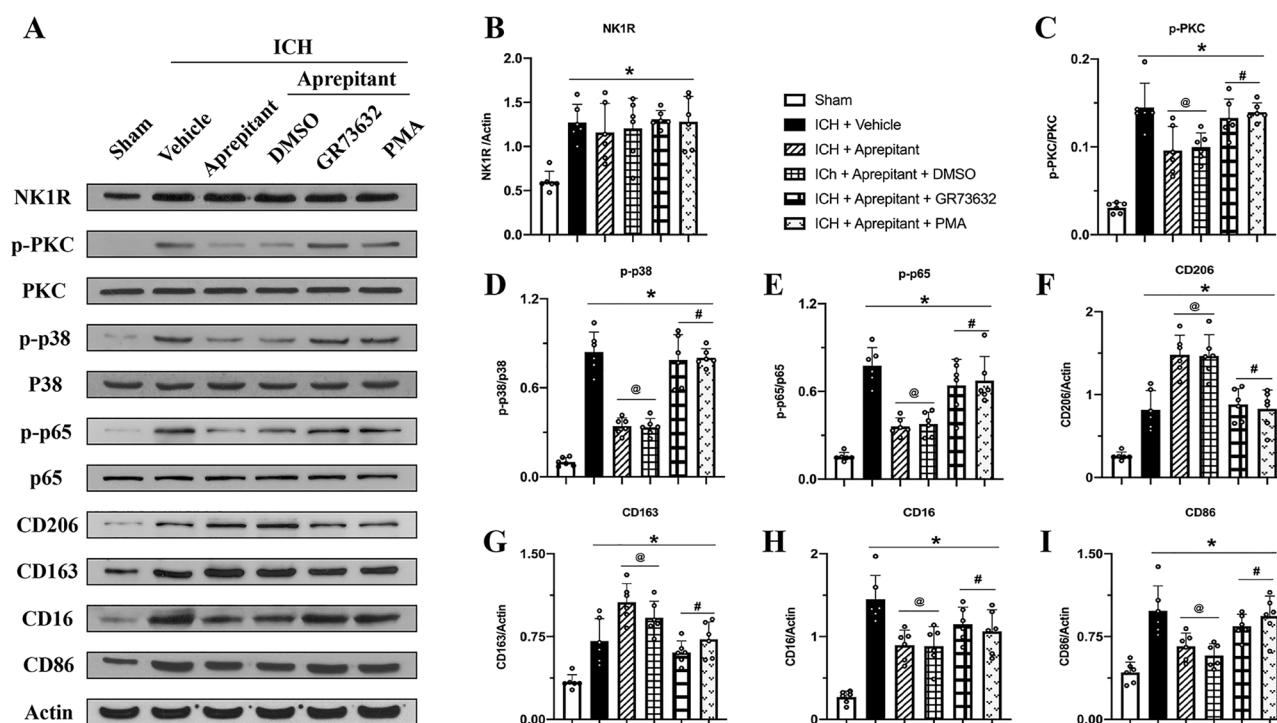


Fig. 7 Activation of NK1R or PKC abolished the effects of Aprepitant after ICH. **A** Representative western blot bands; **B–I** quantitative analyses of NK1R, p-PKC/PKC, p-P38/P38MAPK, p-P65/P65 NF κ B, CD206, CD163, CD16, and CD86 in the ipsilateral

hemisphere at 72 h after ICH. Data was represented as mean \pm SD. * p < 0.05 vs Sham, @ p < 0.05 vs ICH + vehicle, # p < 0.05 vs ICH + Aprepitant + DMSO; one-way ANOVA, Tukey post hoc test, n = 6/group

We explored downstream orchestrators of NK1R activation to determine potential mechanisms for hematoma clearance. We specifically focused on the SP/NK1R downstream signaling pathway that mediated microglia M2 polarization. It has been previously shown that SP upon binding to NK1R activates PLC, which leads to the formation of inositol triphosphate and diacylglycerol, which then activates PKC [13]. Phosphorylated PKC can activate members of the MAPK cascade, including extracellular signal-regulated kinases 1 and 2, as well as p38MAPK, thereby activating NF κ B [22]. Furthermore, previous studies have indicated that NK1R can activate NF κ B signaling [48], and SP-induced NF κ B activation required p38MAPK in macrophages [49]. Another study similarly showed that inhibition of NK1R signaling reduced NF κ B activation, thereby decreasing TNF- α and IL-1 β expression in lipopolysaccharide (LPS)-induced macrophages [50]. Likewise, in the current study, we found that NK1R antagonist Aprepitant significantly reduced PKC/p38MAPK/NF κ B expression in ICH mice that received Aprepitant treatment. The NF κ B pathway is known to play a crucial role in microglial polarization. In vitro, inhibition of TLR4/NF κ B signaling promoted LPS-stimulated transition of microglia from M1 to M2 phenotype [51]. In vivo studies have likewise confirmed the relationship between NF κ B signaling and microglial polarization [52].

Microglial phenotype modulation is potentially an important target for the treatment of ICH, since M2-like microglia may promote phagocytosis of erythrocytes and tissue debris, thereby contributing to the clearance of hematoma [9]. Consistent with previous studies [53], our double immunofluorescence results showed that both M1 and M2 microglia were elevated in the acute phase at 3 days following ICH with the M1 phenotype predominantly elevated. However, Aprepitant treatment promoted M2 microglia by reducing NF κ B activation, and this translated into hematoma clearance as shown by reduced hematoma volume following ICH.

We also investigated the upstream regulation of NK1R activation after ICH injury. Previous literature demonstrated that thrombin regulated the expression of NK1R endogenous ligand SP through PAR-1 receptor in neurons [14]. Therefore, in the present study, we explored the effects of thrombin-injection in naïve mice to explore the potential relationship between thrombin and SP/NK1R system. In naïve mice, we found that thrombin injection significantly increased SP expression, and the administration of a thrombin-specific inhibitor hirudin significantly down-regulated SP and was accompanied by a greater shift of microglia to M2 phenotype. Likewise, Aprepitant administration to naïve mice with thrombin injection showed a similar effect towards M2 phenotype but did not alter SP expression.

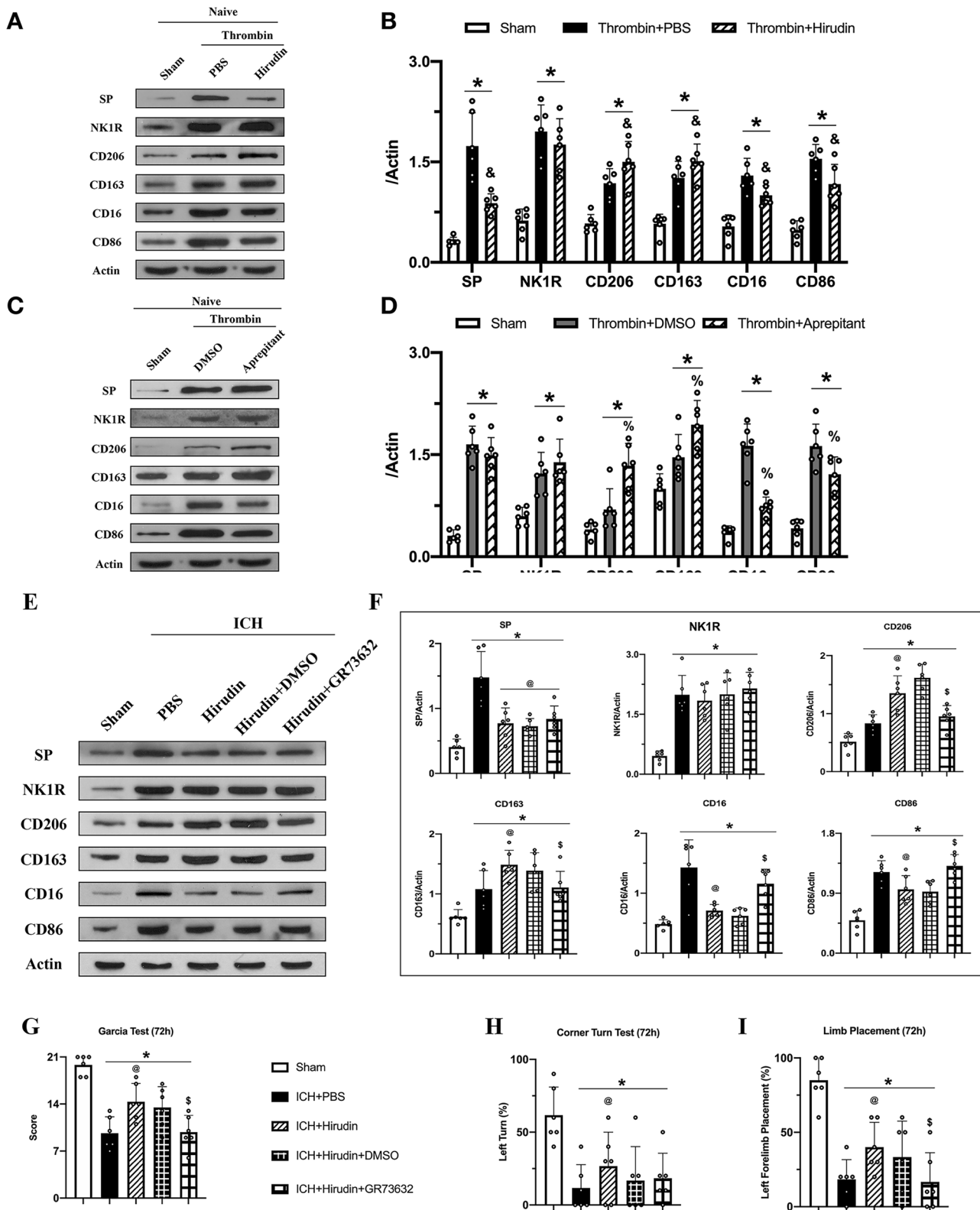


Fig. 8 Thrombin regulated NK1R activation by promoting substance P release and effects of hirudin was reversed by NK1R agonist GR73632. **A, C, E** Representative western blot bands; **B, D, F** quantitative analyses of substance P (SP), NK1R, CD206, CD163, CD16, and CD86 in the ipsilateral hemisphere at 72 h after surgery;

G modified Garcia test; **H** corner turn test; and **I** forelimb placement test at 72 h after ICH. Data was represented as mean \pm SD. * $p < 0.05$ vs Sham, & $p < 0.05$ vs thrombin+PBS, % $p < 0.05$ vs thrombin+DMSO; @ $p < 0.05$ vs ICH+PBS, \$ $p < 0.05$ vs ICH+Hirudin+DMSO, one-way ANOVA, Tukey post hoc test, $n = 6/\text{group}$

Furthermore, in an autologous blood injection ICH model, we found that hirudin reduced SP expression and promoted M2 microglia, and the NK1R agonist GR73632 reversed the protective effects of hirudin. These results suggested that following ICH, thrombin may exert harmful effects through NK1R activation. Thrombin may therefore be one of the upstream regulators of NK1R activation. Although a series of studies have shown that thrombin inhibition can exert neuroprotective effects in animal models [54, 55], clinical trials have shown that thrombin inhibition can have adverse effects including increased bleeding [56, 57, 58]. Therefore, interfering with the downstream effectors of thrombin may be a reasonable therapeutic strategy. Our study provides new options for the treatment of ICH and thrombin-induced brain damage by targeting NK1R activation.

As research on NK1R has intensified, several NK1R-specific inhibitors have been developed. To make it easier to translate our findings for clinical application, in this study, we chose Aprepitant which is the first NK1R-specific antagonist approved by FDA for the treatment of chemotherapy-induced nausea and vomiting [59]. Aprepitant can cross the blood–brain barrier and competitively bind to NK1R receptors in the brain antagonizing the effects of the natural ligand SP [60]. Furthermore, Aprepitant had neuroprotective effects in ischemic brain injury model and it also reduced blood–brain barrier dysfunction and edema formation in an experimental model of brain tumors [20, 61]. In our study, we observed that Aprepitant reduced brain edema, promoted hematoma clearance, and improved neurological function in ICH mice. Our long-term neurobehavioral experiments and Nissl staining results showed that Aprepitant reduced neuronal degeneration and improved learning, cognitive, and memory deficits in mice after ICH. The long-term improvement may be the beneficial effects of hematoma clearance in the first 7 days after ICH, as erythrocytes not phagocytosed by microglia/macrophages may lyse, releasing potentially harmful components such as hemoglobin and iron into the extracellular space [62]. These harmful substances, in turn, may affect the survival of hippocampal neurons through the circulation of cerebrospinal fluid. Additionally, NK1R is also expressed on the surface of neurons, and part of the protective effects of Aprepitant may be due to direct effects on neurons. Investigating the effect of Aprepitant treatment on neuronal survival is a future research direction.

It is important to note that there are some limitations in the present study. First, previous studies showed that inhibition of NK1R exerted anti-inflammatory effects and blood–brain barrier protection [18, 47]. In this study, we focused on the role of NK1R in microglial polarization. Therefore, further exploration of other neuroprotective roles of NK1R after ICH is needed. Second, NK1R downstream pathways also include AC/cAMP/PKA and Rho/ROCK [21], which have been shown to play a role in regulating

microglial polarization [63, 64]. Our study focused on the PKC/p38MAPK/NFκB pathway as a potential mechanism. Therefore, we need to further elucidate the NK1R downstream signaling pathways. Lastly, only male mice were used for the study and sex differences were not examined, which is another limitation of the study.

Conclusions

In conclusion, our results demonstrated that SP/NK1R contributed to microglia polarization and hematoma clearance after ICH, at least partly, through PKC/p38MAPK/NFκB signaling pathway. Thrombin, an established mediator of brain injury, may be an upstream regulator of NK1R activation by promoting SP release. Most importantly we also demonstrated that Aprepitant, a selective NK1R antagonist, enhanced hematoma clearance, attenuated brain injury, and improved short-term and long-term outcomes in ICH mice. Considering that Aprepitant is an FDA-approved, well-tolerated drug, our findings may provide new strategies for the treatment of ICH patients.

Supplementary Information The online version contains supplementary material available at <https://doi.org/10.1007/s13311-021-01077-8>.

Author Contribution This study was designed by PJ, PS, LH, JHZ, YG, and JT. The experiments were completed by PJ, SXD, YHC, GGL, LFL, SCX, and LC. PJ, SXD, and YHC performed statistical analysis. PJ, SXD, DTZ, and PS finished writing the manuscript. YG and JT provided supervision and final check. All the authors read the final version of this paper and approved it.

Funding This study was supported by grants from the National Institutes of Health (R01NS091042 to John H. Zhang) and the National Key R&D Program of China (2018YFC1312600 and 2018YFC1312604 to Ye Gong), and the Science and Technology Commission of Shanghai Municipal (18140901100 to Ye Gong).

Declarations

Competing Interests The authors declare no competing interests.

References

1. Liddle LJ, Ralhan S, Ward DL, Colbourne F. Translational Intracerebral Hemorrhage Research: Has Current Neuroprotection Research ARRIVED at a Standard for Experimental Design and Reporting? *Transl Stroke Res*. 2020.
2. Schrag M, Kirshner H. Management of Intracerebral Hemorrhage: JACC Focus Seminar. *J Am Coll Cardiol*. 2020;75(15):1819-31.
3. Liddle LJ, Ralhan S, Ward DL, Colbourne F. Translational Intracerebral Hemorrhage Research: Has Current Neuroprotection Research ARRIVED at a Standard for Experimental Design and Reporting? *Transl Stroke Res*. 2020;11(6):1203-13.

4. Corbett D, Carmichael ST, Murphy TH, Jones TA, Schwab ME, Jolkkonen J, et al. Enhancing the Alignment of the Preclinical and Clinical Stroke Recovery Research Pipeline: Consensus-Based Core Recommendations From the Stroke Recovery and Rehabilitation Roundtable Translational Working Group. *Neurorehabil Neural Repair*. 2017;31(8):699-707.
5. Zhuang J, Peng Y, Gu C, Chen H, Lin Z, Zhou H, et al. Wogonin Accelerates Hematoma Clearance and Improves Neurological Outcome via the PPAR-gamma Pathway After Intracerebral Hemorrhage. *Transl Stroke Res*. 2020.
6. Broderick JP, Brott TG, Duldner JE, Tomsick T, Huster G. Volume of intracerebral hemorrhage. A powerful and easy-to-use predictor of 30-day mortality. *Stroke*. 1993;24(7):987-93.
7. Van Asch CJ, Luitse MJ, Rinkel GJ, van der Tweel I, Algra A, Klijn CJ. Incidence, case fatality, and functional outcome of intracerebral haemorrhage over time, according to age, sex, and ethnic origin: a systematic review and meta-analysis. *Lancet Neurol*. 2010;9(2):167-76.
8. Hanley DF, Thompson RE, Rosenblum M, Yenokyan G, Lane K, McBee N, et al. Efficacy and safety of minimally invasive surgery with thrombolysis in intracerebral haemorrhage evacuation (MISTIE III): a randomised, controlled, open-label, blinded endpoint phase 3 trial. *Lancet*. 2019;393(10175):1021-32.
9. Lan X, Han X, Li Q, Yang QW, Wang J. Modulators of microglial activation and polarization after intracerebral haemorrhage. *Nat Rev Neurol*. 2017;13(7):420-33.
10. Hu R, Zhang C, Xia J, Ge H, Zhong J, Fang X, et al. Long-term Outcomes and Risk Factors Related to Hydrocephalus After Intracerebral Hemorrhage. *Transl Stroke Res*. 2020.
11. Mashaghi A, Marmalidou A, Tehrani M, Grace PM, Pothoulakis C, Dana R. Neuropeptide substance P and the immune response. *Cell Mol Life Sci*. 2016;73(22):4249-64.
12. US VE, Gaddum JH. An unidentified depressor substance in certain tissue extracts. *J Physiol*. 1931;72(1):74-87.
13. Suvas S. Role of Substance P Neuropeptide in Inflammation, Wound Healing, and Tissue Homeostasis. *J Immunol*. 2017;199(5):1543-52.
14. De Garavilla L, Vergnolle N, Young SH, Ennes H, Steinhoff M, Ossovskaya VS, et al. Agonists of proteinase-activated receptor 1 induce plasma extravasation by a neurogenic mechanism. *Br J Pharmacol*. 2001;133(7):975-87.
15. Monastyrskaya K, Hostettler A, Buergi S, Draeger A. The NK1 receptor localizes to the plasma membrane microdomains, and its activation is dependent on lipid raft integrity. *J Biol Chem*. 2005;280(8):7135-46.
16. Martinez AN, Philipp MT. Substance P and Antagonists of the Neurokinin-1 Receptor in Neuroinflammation Associated with Infectious and Neurodegenerative Diseases of the Central Nervous System. *J Neurol Neuromedicine*. 2016;1(2):29-36.
17. Nessler S, Stadelmann C, Bittner A, Schlegel K, Gronen F, Brueck W, et al. Suppression of autoimmune encephalomyelitis by a neurokinin-1 receptor antagonist--a putative role for substance P in CNS inflammation. *J Neuroimmunol*. 2006;179(1-2):1-8.
18. Li Q, Wu X, Yang Y, Zhang Y, He F, Xu X, et al. Tachykinin NK1 receptor antagonist L-733,060 and substance P deletion exert neuroprotection through inhibiting oxidative stress and cell death after traumatic brain injury in mice. *Int J Biochem Cell Biol*. 2019;107:154-65.
19. Ansar S, Svendgaard NA, Edvinsson L. Neurokinin-1 receptor antagonism in a rat model of subarachnoid hemorrhage: prevention of upregulation of contractile ETB and 5-HT1B receptors and cerebral blood flow reduction. *J Neurosurg*. 2007;106(5):881-6.
20. Kaur J, Sharma S, Sandhu M, Sharma S. Neurokinin-1 receptor inhibition reverses ischaemic brain injury and dementia in bilateral common carotid artery occluded rats: possible mechanisms. *Inflammopharmacology*. 2016;24(4):133-43.
21. Steinhoff MS, von Mentzer B, Geppetti P, Pothoulakis C, Bunnett NW. Tachykinins and their receptors: contributions to physiological control and the mechanisms of disease. *Physiol Rev*. 2014;94(1):265-301.
22. Johnson MB, Young AD, Marriott I. The Therapeutic Potential of Targeting Substance P/NK-1R Interactions in Inflammatory CNS Disorders. *Front Cell Neurosci*. 2016;10:296.
23. Yao K, Zu HB. Microglial polarization: novel therapeutic mechanism against Alzheimer's disease. *Inflammopharmacology*. 2020;28(1):95-110.
24. Yan J, Zuo G, Sherchan P, Huang L, Ocak U, Xu W, et al. CCR1 Activation Promotes Neuroinflammation Through CCR1/TPR1/ERK1/2 Signaling Pathway After Intracerebral Hemorrhage in Mice. *Neurotherapeutics*. 2020.
25. Rynkowski MA, Kim GH, Komotar RJ, Otten ML, Ducruet AF, Zacharia BE, et al. A mouse model of intracerebral hemorrhage using autologous blood infusion. *Nat Protoc*. 2008;3(1):122-8.
26. Millan MJ, Dekeyne A, Gobert A, Mannoury la Cour C, Brocco M, Rivet JM, et al. S41744, a dual neurokinin (NK)1 receptor antagonist and serotonin (5-HT) reuptake inhibitor with potential antidepressant properties: a comparison to aprepitant (MK869) and paroxetine. *Eur Neuropsychopharmacol*. 2010;20(9):599-621.
27. Di T, Zhang S, Hong J, Zhang T, Chen L. Hyperactivity of Hypothalamic-Pituitary-Adrenal Axis Due to Dysfunction of the Hypothalamic Glucocorticoid Receptor in Sigma-1 Receptor Knockout Mice. *Front Mol Neurosci*. 2017;10:287.
28. Bai Q, Shao J, Cao J, Ren X, Cai W, Su S, et al. Protein kinase C-alpha upregulates sodium channel Nav1.9 in nociceptive dorsal root ganglion neurons in an inflammatory arthritis pain model of rat. *J Cell Biochem*. 2020;121(1):768-78.
29. Wang G, Guo Z, Tong L, Xue F, Krafft PR, Budbazar E, et al. TLR7 (Toll-Like Receptor 7) Facilitates Heme Scavenging Through the BTK (Bruton Tyrosine Kinase)-CRT (Calreticulin)-LRP1 (Low-Density Lipoprotein Receptor-Related Protein-1)-Hx (Hemopexin) Pathway in Murine Intracerebral Hemorrhage. *Stroke*. 2018;49(12):3020-9.
30. Chen S, Zuo Y, Huang L, Sherchan P, Zhang J, Yu Z, et al. The MC4 receptor agonist RO27-3225 inhibits NLRP1-dependent neuronal pyroptosis via the ASK1/JNK/p38 MAPK pathway in a mouse model of intracerebral haemorrhage. *Br J Pharmacol*. 2019;176(9):1341-56.
31. Ma Q, Huang B, Khatibi N, Rolland W, 2nd, Suzuki H, Zhang JH, et al. PDGFR-alpha inhibition preserves blood-brain barrier after intracerebral hemorrhage. *Ann Neurol*. 2011;70(6):920-31.
32. Manaenko A, Yang P, Nowrangi D, Budbazar E, Hartman RE, Obenaus A, et al. Inhibition of stress fiber formation preserves blood-brain barrier after intracerebral hemorrhage in mice. *J Cereb Blood Flow Metab*. 2018;38(1):87-102.
33. Chen S, Peng J, Sherchan P, Ma Y, Xiang S, Yan F, et al. TREM2 activation attenuates neuroinflammation and neuronal apoptosis via PI3K/Akt pathway after intracerebral hemorrhage in mice. *J Neuroinflammation*. 2020;17(1):168.
34. Rolland WB, Lekic T, Krafft PR, Hasegawa Y, Altay O, Hartman R, et al. Fingolimod reduces cerebral lymphocyte infiltration in experimental models of rodent intracerebral hemorrhage. *Exp Neurol*. 2013;241:45-55.
35. Mo J, Enkhjargal B, Travis ZD, Zhou K, Wu P, Zhang G, et al. AVE 0991 attenuates oxidative stress and neuronal apoptosis via Mas/PKA/CREB/UCP-2 pathway after subarachnoid hemorrhage in rats. *Redox Biol*. 2019;20:75-86.
36. Lu Z, Wang Z, Yu L, Ding Y, Xu Y, Xu N, et al. GCN2 reduces inflammation by p-eIF2alpha/ATF4 pathway after intracerebral hemorrhage in mice. *Exp Neurol*. 2019;313:16-25.

37. Chang CF, Cai L, Wang J. Translational intracerebral hemorrhage: a need for transparent descriptions of fresh tissue sampling and preclinical model quality. *Transl Stroke Res.* 2015;6(5):384-9.
38. Fu P, Liu J, Bai Q, Sun X, Yao Z, Liu L, et al. Long-term outcomes of monascin - a novel dual peroxisome proliferator-activated receptor gamma/nuclear factor-erythroid 2 related factor-2 agonist in experimental intracerebral hemorrhage. *Ther Adv Neurol Disord.* 2020;13:1756286420921083.
39. Towbin H, Staehelin T, Gordon J. Electrophoretic transfer of proteins from polyacrylamide gels to nitrocellulose sheets: procedure and some applications. *Proc Natl Acad Sci U S A.* 1979;76(9):4350-4.
40. Xiao N, Liu TL, Li H, Xu HC, Ge J, Wen HY, et al. Low Serum Uric Acid Levels Promote Hypertensive Intracerebral Hemorrhage by Disrupting the Smooth Muscle Cell-Elastin Contractile Unit and Upregulating the Erk1/2-MMP Axis. *Transl Stroke Res.* 2020.
41. Doycheva D, Xu N, Kaur H, Malaguit J, McBride DW, Tang J, et al. Adenoviral TMBIM6 vector attenuates ER-stress-induced apoptosis in a neonatal hypoxic-ischemic rat model. *Dis Model Mech.* 2019;12(11).
42. Chen JX, Wang YP, Zhang X, Li GX, Zheng K, Duan CZ. lncRNA Mtss1 promotes inflammatory responses and secondary brain injury after intracerebral hemorrhage by targeting miR-709 in mice. *Brain Res Bull.* 2020;162:20-9.
43. Chen CJ, Ding D, Ironside N, Buell TJ, Elder LJ, Warren A, et al. Statins for neuroprotection in spontaneous intracerebral hemorrhage. *Neurology.* 2019;93(24):1056-66.
44. Zhao X, Sun G, Zhang J, Strong R, Song W, Gonzales N, et al. Hematoma resolution as a target for intracerebral hemorrhage treatment: role for peroxisome proliferator-activated receptor gamma in microglia/macrophages. *Ann Neurol.* 2007;61(4):352-62.
45. Xi G, Keep RF, Hoff JT. Mechanisms of brain injury after intracerebral haemorrhage. *Lancet Neurol.* 2006;5(1):53-63.
46. Chauhan VS, Sterka DG, Jr., Gray DL, Bost KL, Marriott I. Neurogenic exacerbation of microglial and astrocyte responses to *Neisseria meningitidis* and *Borrelia burgdorferi*. *J Immunol.* 2008;180(12):8241-9.
47. Yu Y, Zhu W, Liang Q, Liu J, Yang X, Sun G. Tropisetron attenuates lipopolysaccharide induced neuroinflammation by inhibiting NF-kappaB and SP/NK1R signaling pathway. *J Neuroimmunol.* 2018;320:80-6.
48. Fiebich BL, Schleicher S, Butcher RD, Craig A, Lieb K. The neuropeptide substance P activates p38 mitogen-activated protein kinase resulting in IL-6 expression independently from NF-kappa B. *J Immunol.* 2000;165(10):5606-11.
49. Sun J, Ramnath RD, Zhi L, Tamizhselvi R, Bhatia M. Substance P enhances NF-kappaB transactivation and chemokine response in murine macrophages via ERK1/2 and p38 MAPK signaling pathways. *Am J Physiol Cell Physiol.* 2008;294(6):C1586-96.
50. Xu J, Xu F, Lin Y. Cigarette smoke synergizes lipopolysaccharide-induced interleukin-1beta and tumor necrosis factor-alpha secretion from macrophages via substance P-mediated nuclear factor-kappaB activation. *Am J Respir Cell Mol Biol.* 2011;44(3):302-8.
51. Slusarczyk J, Trojan E, Glombik K, Piotrowska A, Budziszewska B, Kubera M, et al. Targeting the NLRP3 Inflammasome-Related Pathways via Tianeptine Treatment-Suppressed Microglia Polarization to the M1 Phenotype in Lipopolysaccharide-Stimulated Cultures. *Int J Mol Sci.* 2018;19(7).
52. Popiolek-Barczyk K, Kolosowska N, Piotrowska A, Makuch W, Rojewska E, Jurga AM, et al. Parthenolide Relieves Pain and Promotes M2 Microglia/Macrophage Polarization in Rat Model of Neuropathy. *Neural Plast.* 2015;2015:676473.
53. Kigerl KA, Gensel JC, Ankeny DP, Alexander JK, Donnelly DJ, Popovich PG. Identification of two distinct macrophage subsets with divergent effects causing either neurotoxicity or regeneration in the injured mouse spinal cord. *J Neurosci.* 2009;29(43):13435-44.
54. Kitaoka T, Hua Y, Xi G, Hoff JT, Keep RF. Delayed argatroban treatment reduces edema in a rat model of intracerebral hemorrhage. *Stroke.* 2002;33(12):3012-8.
55. Xue M, Fan Y, Liu S, Zygun DA, Demchuk A, Yong VW. Contributions of multiple proteases to neurotoxicity in a mouse model of intracerebral haemorrhage. *Brain.* 2009;132(Pt 1):26-36.
56. Matsuoka H, Hamada R. Role of thrombin in CNS damage associated with intracerebral haemorrhage: opportunity for pharmacological intervention? *CNS Drugs.* 2002;16(8):509-16.
57. Hursting MJ, Alford KL, Becker JC, Brooks RL, Joffrion JL, Knappenberger GD, et al. Novastan (brand of argatroban): a small-molecule, direct thrombin inhibitor. *Semin Thromb Hemost.* 1997;23(6):503-16.
58. Ye F, Garton HJL, Hua Y, Keep RF, Xi G. The Role of Thrombin in Brain Injury After Hemorrhagic and Ischemic Stroke. *Transl Stroke Res.* 2020.
59. Murakami C, Kakuta N, Satomi S, Nakamura R, Miyoshi H, Morio A, et al. [Neurokinin-1 receptor antagonists for postoperative nausea and vomiting: a systematic review and meta-analysis]. *Rev Bras Anesthesiol.* 2020.
60. Rizk AN, Hesketh PJ. Antiemetics for cancer chemotherapy-induced nausea and vomiting. A review of agents in development. *Drugs R D.* 1999;2(4):229-35.
61. Harford-Wright E, Lewis KM, Ghabriel MN, Vink R. Treatment with the NK1 antagonist emend reduces blood brain barrier dysfunction and edema formation in an experimental model of brain tumors. *PLoS One.* 2014;9(5):e97002.
62. Wilkinson DA, Keep RF, Hua Y, Xi G. Hematoma clearance as a therapeutic target in intracerebral hemorrhage: From macro to micro. *J Cereb Blood Flow Metab.* 2018;38(4):741-5.
63. Dyck S, Kataria H, Alizadeh A, Santhosh KT, Lang B, Silver J, et al. Perturbing chondroitin sulfate proteoglycan signaling through LAR and PTPsigma receptors promotes a beneficial inflammatory response following spinal cord injury. *J Neuroinflammation.* 2018;15(1):90.
64. Tao Y, Li L, Jiang B, Feng Z, Yang L, Tang J, et al. Cannabinoid receptor-2 stimulation suppresses neuroinflammation by regulating microglial M1/M2 polarization through the cAMP/PKA pathway in an experimental GMH rat model. *Brain Behav Immun.* 2016;58:118-29.

Publisher's Note Springer Nature remains neutral with regard to jurisdictional claims in published maps and institutional affiliations.